

## Author's Accepted Manuscript

A novel sensitive amperometric choline biosensor based on multiwalled carbon nanotubes and gold nanoparticles

Hend Samy Magar, Mariana Emilia Ghica, Mohammed Nooredeen Abbas, Christopher M.A. Brett



[www.elsevier.com/locate/talanta](http://www.elsevier.com/locate/talanta)

PII: S0039-9140(17)30262-X  
DOI: <http://dx.doi.org/10.1016/j.talanta.2017.02.048>  
Reference: TAL17324

To appear in: *Talanta*

Received date: 29 December 2016  
Revised date: 17 February 2017  
Accepted date: 19 February 2017

Cite this article as: Hend Samy Magar, Mariana Emilia Ghica, Mohammed Nooredeen Abbas and Christopher M.A. Brett, A novel sensitive amperometric choline biosensor based on multiwalled carbon nanotubes and gold nanoparticles *Talanta*, <http://dx.doi.org/10.1016/j.talanta.2017.02.048>

This is a PDF file of an unedited manuscript that has been accepted for publication. As a service to our customers we are providing this early version of the manuscript. The manuscript will undergo copyediting, typesetting, and review of the resulting galley proof before it is published in its final citable form. Please note that during the production process errors may be discovered which could affect the content, and all legal disclaimers that apply to the journal pertain.

## A novel sensitive amperometric choline biosensor based on multiwalled carbon nanotubes and gold nanoparticles

Hend Samy Magar<sup>a,b</sup>, Mariana Emilia Ghica<sup>b</sup>, Mohammed Nooredeen Abbas<sup>a</sup>, Christopher M.A. Brett<sup>b,\*</sup>

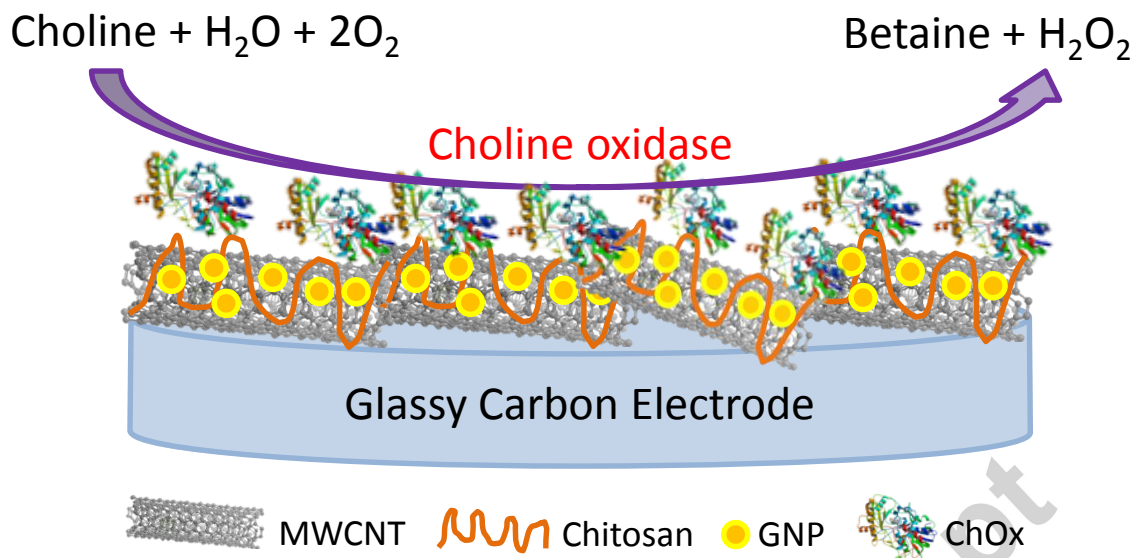
<sup>a</sup>*Applied Organic Chemistry Department, National Research Centre, Giza, Egypt.*

<sup>b</sup>*Department of Chemistry, Faculty of Sciences and Technology, University of Coimbra, 3004-535 Coimbra, Portugal.*

\*Corresponding author: Tel: +351-239854470; Fax: +351-239827703. E-mail: cbrett@ci.uc.pt

### Abstract

A novel amperometric biosensor for choline determination has been developed, exploiting the electrocatalytic properties of multiwalled carbon nanotubes (MWCNT) and gold nanoparticles (GNP). Chitosan (Chit), a natural biocompatible polymer, was used to disperse CNT, then Chit-MWCNT was dropped on the surface of a glassy carbon electrode (GCE), followed by GNP; finally, choline oxidase (ChOx) was immobilized by glutaraldehyde crosslinking. The ChOx/(GNP)<sub>4</sub>/MWCNT/GCE exhibited linear response to choline from 3 to 120  $\mu\text{M}$ , the sensitivity was  $204 \mu\text{A cm}^{-2} \text{mM}^{-1}$  and the detection limit was  $0.6 \mu\text{M}$ . The biosensor exhibited good intra and inter-electrode precision, and excellent selectivity and stability. Electrochemical impedance spectroscopy (EIS) was also used to measure choline at  $0.0 \text{ V}$  and this is the first report on choline determination by EIS. Successful measurement in milk samples was performed.



### Keywords:

choline biosensor; choline oxidase; multiwalled carbon nanotubes; gold nanoparticles; electrochemical impedance spectroscopy

### 1. Introduction

Choline is a vital nutrient [1], required for many physiological purposes. It is a precursor of the neurotransmitter acetylcholine, which is involved in memory and muscle control [2], it is a major source of methyl groups via its metabolite, betaine [3], and it is important in the synthesis of some essential phospholipids that provide structure to cell membranes and facilitate transmembrane signalling [4]. Therefore, the quantitative determination of choline is important in clinical analysis, especially in the early diagnosis of brain disorders such as Alzheimer's and Parkinson's diseases [5]. Among the different methods available for choline

detection, amperometric biosensors based on choline oxidase (ChOx) present advantages such as simplicity, reliability, rapid response, high sensitivity and low cost [6]. The physical and chemical properties of the materials used in the construction of biosensors have a significant influence on their performance. Different configurations have been used for choline biosensors including redox mediators [6-8], conducting polymers [1], carbon nanotubes [9-11], graphene [12], nanoparticles [13], and their combinations [12,14-16]. In most of the cases the measurement is based on the amperometric detection of hydrogen peroxide ( $H_2O_2$ ), a side product of the choline oxidase catalysed reaction;  $H_2O_2$  reacts either directly with the redox mediator [6-8,10], or its reaction is catalysed by a second enzyme, horseradish peroxidase, in order to increase the signal [12,17]. Nevertheless, there are also reports of direct electronic communication between ChOx and electrodes [11,18].

The inclusion of carbon nanotubes, usually multiwalled carbon nanotubes (MWCNT) in enzyme-based biosensors has attracted the attention of many researchers due to their unique physical and chemical properties, which provide high surface area for enzyme loading and a compatible micro-environment; their ability to promote electron transfer between the biomolecules and the electrode surface has been extensively studied [19-21]. Gold nanoparticles (GNP) are one of the most extensively studied and used metal nanoparticles in amperometric biosensors, owing to their stable physical and chemical properties, catalytic activity, due to their small size [21-23]. A mixture of MWCNT and GNP has been shown to be an effective approach to enhance the properties of biosensors [19,24-26]. Only two configurations comprising both MWCNT and GNP together with ChOx were found in the literature [27,28], one of them additionally containing poly(diallyldimethylammonium chloride) (PDDA) [28].

Electrochemical impedance spectroscopy (EIS) is a rapidly developing technique for the study of sensing events at the surface of the electrodes and is widely used in different fields,

e.g. [29-31]. Faradaic impedimetric systems are based on measuring the charge transfer resistance of a redox probe at electrode interface. Impedance detection has been found to be sensitive, rapid and with low detection limit. Moreover, the measurement does not have any specific prerequisites (e.g., labels or electroactive moieties in the molecule) [31]. Impedimetric determination of acetylcholine has been performed [32]; however, choline determination by EIS has not been previously reported.

The aim of this work was to develop a novel electrochemical biosensor for the quantitative detection of choline. For this purpose, a comprehensive investigation of choline oxidation at the enzyme-modified electrode was carried out by amperometric and impedimetric methods at different applied potentials. Experimental parameters were optimized and the amperometric performance compared with other choline biosensors. Different electrode architectures were investigated by fixed potential amperometry and EIS for choline determination. This study presents the first impedimetric electrochemical detection of choline with nanostructured enzyme modified electrodes and shows good response at 0.0 V vs Ag/AgCl.

## 2. Experimental

### 2.1 Reagents

Choline oxidase (ChOx, from *Alcaligenes sp.*, 14 U/mg), choline chloride, chitosan (Chit) of low molecular weight with a degree of deacetylation of 80 %, bovine serum albumin (BSA), glutaraldehyde (GA, 25% v/v in water) and gold (III) chloride hydrate were acquired from Sigma Aldrich. Multi-walled carbon nanotubes (MWCNT) with ~95% purity, 30±10 nm diameter and 1-5 µm length were from Nanolab, U.S.A. Sodium chloride (NaCl), sodium hydrogenphosphate and sodium dihydrogenphosphate (Na<sub>2</sub>HPO<sub>4</sub> and NaH<sub>2</sub>PO<sub>4</sub>) were from Riedel-de-Haën and trisodium citrate, was obtained from Merck. Sodium phosphate buffer

saline (NaPBS) obtained by adding 0.05 M NaCl to 0.1 M phosphate buffer (0.1 M Na<sub>2</sub>HPO<sub>4</sub>/NaH<sub>2</sub>PO<sub>4</sub>) was used in all studies.

All solutions were prepared with Millipore MilliQ ultrapure water (resistivity > 18 MΩ cm) and experiments were performed at room temperature (25 ± 1 °C).

## 2.2. Apparatus and measurements

The electrochemical amperometric experiments were performed using an Ivium CompactStat potentiostat (Ivium Technologies). EIS experiments were carried out with a potentiostat/galvanostat/ZRA (Gamry Instruments, Reference 600). A root mean square (rms) perturbation of 10 mV was applied over the frequency range 65 kHz – 0.1 Hz, with 10 frequency values per frequency decade and ZView 2.4 software (Solartron Analytical, UK), was used to fit the spectra to equivalent electrical circuits.

All electrochemical measurements were carried out at room temperature in a conventional three-electrode cell containing a bare or modified glassy carbon electrode (GCE) (EDAQ, ET074-3 Glassy Carbon Disk Electrode), with a diameter of 1 mm, as working electrode, a platinum wire as auxiliary electrode and a Ag/AgCl (3 M KCl) electrode (Metrohm-Autolab) as reference.

Transmission electron microscopy (TEM) images were recorded using a JEOL JEM-1230. UV-Vis spectra were recorded using a SHIMADZU UV-VIS recording spectrophotometer (UV-2401PC).

## 2.3. Preparation of carbon nanotubes (MWCNT) in chitosan solution

The MWCNT were purified and functionalised as previously reported [33] by treating with 5 M HNO<sub>3</sub> for 24 h in order to introduce COOH groups at the end and side wall defects of the nanotube structure [34]. The solution was then filtered and washed with Milli-Q nanopure

water until neutral and finally dried in an oven overnight. A 0.2 % MWCNT solution was prepared by dispersing 1 mg of functionalised MWCNT in 500  $\mu\text{L}$  of a 1 % chitosan solution, previously dissolved in a 1 % acetic acid aqueous solution, and then sonicated for 2 h to ensure complete dissolution and a homogeneous mixture. There is formation of bonds between the amino groups of chitosan and the carboxylic groups of the MWCNT, as described in [33].

#### *2.4. Preparation of gold nanoparticles (GNP)*

GNP were prepared by modifying a previously described procedure [35]. A volume of 400  $\mu\text{L}$  of 40 mM  $\text{HAuCl}_4$  solution was added to 50 mL of distilled water to prepare a 0.01% (w/v) solution. The solution was heated until boiling, then 2 mL of 1% (w/v) trisodium citrate was added rapidly under vigorous stirring. The colour changed from pale yellow to nearly red. The reaction solution was cooled at room temperature and stored at 4  $^{\circ}\text{C}$ . The concentration of the prepared stock solution of GNP was 63  $\text{mg L}^{-1}$ .

### 2.5. Preparation of the modified electrodes

Before each modification, the GCE was polished with alumina slurry. The electrodes were then thoroughly rinsed with ultrapure water and allowed to dry at room temperature. The MWCNT/GCE were prepared by casting 1  $\mu\text{L}$  of 0.2 % MWCNT in chitosan solution on the surface of the GCE and leaving to dry at room temperature. For GNP/MWCNT/GCE, 2 or 4 drops of 1  $\mu\text{L}$  of GNP were successively added on top of the MWCNT/GCE and allowed to dry after each drop, ca. 30 min. In this way, (GNP)<sub>2</sub>/MWCNT/GCE or (GNP)<sub>4</sub>/MWCNT/GCE were formed. Graphene-modified electrodes were also prepared by using 1  $\mu\text{L}$  of either 1.0 % graphene oxide (GO) – GO/GCE or 1.0 % reduced graphene (RG) – RG/GCE. Finally, 1  $\mu\text{L}$  of enzyme solution containing BSA and ChOx was dropped on the surface of the modified electrodes and immediately 1  $\mu\text{L}$  of GA (2.5%) as cross-linking agent between enzyme and BSA, enzyme and chitosan or between two enzyme molecules [33], was added and left to react at room temperature. The schematic biosensor configuration is illustrated in Figure 1. In order to optimize the ChOx concentration, the enzyme solutions were prepared by dissolving different amounts from 10 to 50 mg/mL of ChOx in 0.1 M NaPBS, pH 8.5. For all modifications, the amount of BSA was maintained constant at 40 mg mL<sup>-1</sup>. The modified electrodes were immersed in 0.1 M NaPBS (pH=8.5) and stored at 4 °C overnight.

## 3. Results and discussion

### 3.1. TEM and UV characterization of nanostructures

The nanostructured films formed on the GCE substrate were first characterized by transmission electron microscopy (TEM) and UV-Vis spectrophotometry, Figure 2.



TEM images of MWCNT, Fig.2a1, clearly show the characteristic bundles of these nanostructures with diameter 15-25 nm. In the case of GNP, spherical shapes were observed and the diameter was calculated as  $13.9 \pm 0.4$  nm, Fig. 2a2. TEM was also able to show the distribution of GNP on the surface of the MWCNT. The image in Fig. 2a3 shows that GNP are attached to the ends or to the sidewalls of MWCNT; free nanoparticles are also observed.

UV-Vis spectra, Fig. 2B, show two absorption peaks at 252 and 520 nm, which are characteristic of GNP. For MWCNT, a sharp peak at 218 nm and a shoulder at 296 nm appear. With the addition of GNP to MWCNT the absorption maxima for MWCNT are maintained, but the peak at 252 nm disappeared and the one at 520 nm decreased in intensity, reflecting the attachment of nanoparticles to the nanotubes.

### *3.2. Optimization of the amperometric experimental conditions*

Different parameters were investigated in order to optimise the electrochemical response of the ChOx/(GNP)<sub>4</sub>/MWCNT/GCE biosensor to choline by fixed potential amperometry. These included applied potential, enzyme concentration and pH of the supporting electrolyte.

#### *3.2.1. Influence of potential*

The influence of operating potential on the performance of ChOx/(GNP)<sub>4</sub>/MWCNT/GCE was investigated in 0.1 M NaPBS, pH 8.5. The response to 33  $\mu$ M choline was tested at different potentials between -0.6 and +0.4 V vs. Ag/AgCl, see Fig. 3A. The response increased from -0.6 to -0.5 V and then decreased for less negative potentials; between 0.0 and +0.4 V the response remained almost constant. As a compromise between the highest response and possible response to interferents, a value of -0.3 V was chosen as the working potential for further study.

### 3.2.2. Influence of ChOx concentration

The enzyme concentration can greatly influence the biosensor response. In order to optimise the response to choline, ChOx/(GNP)<sub>4</sub>/MWCNT/GCE biosensors were prepared containing different ChOx loadings, from 10 to 50 mg mL<sup>-1</sup>, while the concentrations of GA and BSA were fixed at 2.5% (v/v) and 40 mg mL<sup>-1</sup>, respectively. The biosensor sensitivity was calculated from slope of the calibration curve, obtained from the amperometric response to choline. The dependence of the sensitivity on enzyme loading is shown in Fig. 3B. It can be clearly seen that the sensitivity of the biosensor improved as the amount of ChOx was increased up to 30 mg mL<sup>-1</sup>, when the highest response was obtained. Increasing enzyme loading above this concentration decreased the sensitivity, probably because of steric hindrance of the enzyme.

### 3.2.3. Influence of pH

The effect of the pH of the buffer solution on the amperometric response of the ChOx/(GNP)<sub>4</sub>/MWCNT/GCE biosensor to 20 μM choline was studied over the range from pH 6.0 to 9.0 in 0.1 M NaPBS. The response was studied at two different applied potentials: -0.3 and +0.4 V, Fig. 3C and the behaviour was similar. The current response increased with increasing pH from 6.0 to 8.5, where the highest amperometric response was obtained, then decreased at pH 9.0. The optimum pH value obtained here is in agreement with that specified by the supplier of the enzyme, and as was previously found for native and immobilised ChOx from *Alcaligenes sp.* in [36].

### 3.3. Analytical performance

Different biosensor configurations were tested, including enzyme with nanotubes, nanoparticles, reduced graphene, graphene oxide and with combinations of nanotubes and nanoparticles and the response to choline investigated. Calibration curves are illustrated in

Fig. 4 for an applied potential of -0.3 V and the analytical parameters are presented in Table 1. There was no response at the electrode modified with reduced graphene and the response at the graphene oxide based biosensor exhibited the lowest sensitivity, this electrode responding only for choline concentrations higher than 100  $\mu\text{M}$ . The highest sensitivity and the lowest detection limit was achieved with the biosensor containing both nanotubes and nanoparticles,  $\text{ChOx}/(\text{GNP})_4/\text{MWCNT}/\text{GCE}$ . This biosensor exhibited a linear response to choline from 3-120  $\mu\text{M}$  with a sensitivity of  $204 \mu\text{A cm}^{-2} \text{mM}^{-1}$  and the limit of detection (LoD) calculated as  $3\text{xSD}/\text{slope}$  was 0.6  $\mu\text{M}$ .

A comparison of the analytical parameters of the fabricated biosensor with other choline biosensors in the literature having similar configurations reported is presented in Table 2. There are only two biosensors with higher sensitivity [10,38]; however, in [38] a more negative potential of -0.5 V was applied, and in [10] the architecture is more complex. The proposed biosensor uses a less negative applied potential (-0.3 V) than other choline biosensors [11,18,38]. The detection limit is not as low as in [16,38], but compares well with others achieved by nanostructured biosensors [10,28,37] and is lower than in [11,35] and particularly 25-fold lower than that obtained with a similar architecture with gold nanoparticles and carbon nanotubes [27].

The relative standard deviation (RSD) for intra-electrode measurements was calculated by measuring the response to 20  $\mu\text{M}$  choline using the same electrode 5 consecutive times, and the value was 1.2 %. The RSD for inter-electrode assays was also calculated, using 3 different electrodes prepared in the same way; and the value was 2.3 %.

### 3.4. Electrochemical impedance spectroscopy

Electrochemical impedance spectroscopy (EIS) has become increasingly used for characterisation of electrochemical sensors and biosensors, e.g. [30,31]. The small-amplitude

perturbation signal makes EIS an excellent tool for indicating changes in the electrical properties of the receptor layer and obtaining information about the ion transport mechanism and characteristics of the electrode interface [39,40]. EIS has been previously used to characterise different stages of electrode modification for choline biosensors [16,37]. However, to our knowledge, there is no report on choline determination by electrochemical impedance spectroscopy.

Impedance spectra were recorded at all the electrode configurations developed, namely ChOx/GO/GCE, ChOx/RG/GCE, ChOx/GNP/GCE, ChOx/MWCNT/GCE and ChOx/GNP/MWCNT/GCE in 0.1 M NaPBS buffer, pH 8.5, at 0.0 V vs Ag/AgCl, Fig. 5A. The spectra obtained are similar, consisting in two semicircles, one in the high frequency region, due to the electrode-modifier film interface and the other for low frequencies, ascribed to the modifier layer-electrolyte interface. All spectra were modelled with the same electrical circuit, Fig. 5B, consisting in a cell resistance,  $R_{\Omega}$ , in series with 2 parallel combinations each consisting of a constant phase element, CPE, and a resistance,  $R$ . The CPE is modelled as a non-ideal capacitor according to the relation  $CPE = -1/(Ci\omega)^{\alpha}$ , where  $C$  is the capacitance (describing the charge separation at the interface),  $\omega$  is the angular frequency and  $\alpha$  is the CPE exponent (due to non-uniformity and roughness of the surface and interfaces).

Values of the fitted equivalent circuit parameters are given in Table 3. The value of  $R_{\Omega}$  was always  $\sim 2.7 \Omega \text{ cm}^2$  for all modified electrodes. The values of the capacitances  $C_1$  and  $C_2$  are higher at the electrodes with MWCNT and with MWCNT and GNP, indicating higher charge accumulation and better conductivity at these electrodes. The values of the charge transfer resistance,  $R_2$ , are the lowest at the same electrodes, showing that the electrons are more easily exchanged for these configurations.

On adding different choline concentrations, the electrodes with reduced graphene exhibited no changes, showing that EIS cannot be used for choline determination in this case; for the other electrodes changes were observed. Due to the fact that the biosensor containing nanotubes and nanoparticles exhibited the lowest impedance value, ChOx/(GNP)<sub>4</sub>/MWCNT/GCE, this modified electrode was used for evaluating the possibility of choline determination by EIS.

Spectra were recorded at different potentials: -0.4, 0.0 and +0.4 V. However, the most significant changes were obtained at 0.0 V and these spectra are shown in Fig. 6A. The values of the parameters obtained are shown in Table 4. The only values with significant changes were those for the resistance from the low frequency region,  $R_2$  as would be expected since this represents the interface that interacts with the analyte directly. No linear dependence was obtained if plotting the values of  $R_2$  versus choline concentration or logarithm of concentration. However, a linear calibration plot could be constructed by plotting the values of  $Z''$  versus logarithm of choline concentration at fixed frequency, chosen as 0.1 Hz, between 1.0 and 500  $\mu$ M, see Fig. 6B.

The results obtained here clearly indicate that EIS can be used for choline determination and has the advantage of using a potential of 0.0 V vs Ag/AgCl, rather than the -0.3 V for fixed potential amperometry. Nevertheless, the logarithmic nature of the calibration plot illustrates its limitation to use as for semi-quantitative determinations.

### 3.5. Storage stability

To investigate the biosensor performance after storage, the amperometric response of the modified electrodes to 10  $\mu$ M choline was tested twice per week, for ChOx/MWCNT/GCE and ChOx/(GNP)<sub>4</sub>/MWCNT/GCE. After one month, a 35 % drop in the response was observed for the electrode having only nanotubes, while the addition of nanoparticles greatly improved the stability, there being only a 7 % decrease. The electrodes developed here

exhibited better stability than most of the choline biosensors reported before [9,10,12,15-17,28] where responses vary between 75.7 % and 90 % after the same tested period. Only two biosensors showed slightly improved stability, 95 % [7] and 94.5 % [37]; however, in [37] two enzymes were used for biosensor preparation: choline oxidase and acetylcholine esterase.

### 3.6. Selectivity

A great drawback of many biosensors in the literature [1,4,5,27] is the high overpotential required for  $H_2O_2$  detection, at which many other electroactive substances in real samples (i.e., ascorbic acid, uric acid, etc.) are electrochemically oxidized, resulting in interfering signals. In order to solve this problem, several approaches have been employed to lower the oxidation potential of  $H_2O_2$ , such as adding horseradish peroxidase [12,17] or redox mediators [6,10,12]. The selectivity of the proposed biosensor was evaluated in the presence of some potential interfering compounds including ascorbic acid, uric acid, dopamine and acetaminophen. For this purpose, the amperometric response of the  $ChOx/(GNP)_4/MWCNT/GCE$  was investigated by successive injection of equal concentrations, 10  $\mu M$ , of choline and interferents. At +0.4 V all these interferents exhibited a high response; however, at -0.3 V there was no change in response from the interfering compounds, demonstrating the high selectivity of the choline biosensor at this applied potential.

### 3.7. Application

To demonstrate its feasibility with natural samples, application of the biosensor to the amperometric determination of choline in 3 different milk samples was performed. Each sample was injected separately into phosphate buffer (pH=8.5) and the concentration was determined using the standard addition method. The results obtained as the average of four

different measurements for each sample were  $0.49\pm 0.15$ ,  $1.39\pm 0.02$  and  $1.59\pm 0.34$  mM, in agreement with those found in other studies [41].

Accepted manuscript

#### 4. Conclusions

A sensitive and selective electrochemical biosensor for the detection of choline has been developed. The synergistic effect of MWCNT and GNP greatly improve the electrode performance. The sensor has been used for the quantitative detection of choline using amperometry and a wide linear range, good intra and inter-electrode precision, and high stability were obtained. The biosensor exhibited a lower detection limit for choline compared with similar biosensors reported in the literature and was used for the determination of choline in milk samples. Electrochemical impedance spectroscopy was successfully used for the first time for semi-quantitative choline detection at an applied potential of 0.0 V.

#### Acknowledgments

The authors gratefully acknowledge the financial support from the European Commission 7<sup>th</sup> Framework Programme Marie Curie Actions People IRSES N°294993 SMARTCANCERSENS and from Fundação para a Ciência e a Tecnologia (FCT), Portugal of projects PTDC/QEQ-QAN/2201/2014, in the framework of Project 3599-PPCDT, and of UID/EMS/00285/2013 (both co-financed by the European Community Fund FEDER). MEG thanks FCT for a postdoctoral fellowship SFRH/BPD/103103/2014.

#### References

- [1] J.J. Langer, M. Filipiak, J. Kecińska, J. Jasnowska, J. Włodarczak, B. Buładowski, Polyaniline biosensor for choline determination, *Surf. Sci.* 573 (2004) 140–145.
- [2] T. Misgeld, R.W. Burgess, R.M. Lewis, J.M. Cunningham, J.W. Lichtman, J.R. Sanes, Roles of neurotransmitter in synapse formation: development of neuromuscular junctions lacking choline acetyltransferase, *Neuron* 36 (2002) 635–648.
- [3] S.H. Zeisel, Choline: Critical role during fetal development and dietary requirements in adults, *Annu. Rev. Nutr.* 26 (2006) 229–250.



- [4] G. Panfili, P. Manzi, D. Compagnone, L. Scarciglia, G. Palleschi, Rapid assay of choline in foods using microwave hydrolysis and a choline biosensor, *J. Agric. Food Chem.* 48 (2000) 3403–3407.
- [5] M. Sánchez-Paniagua López, J.P. Hervás Pérez, E. López-Cabarcos, B. López-Ruiz, Amperometric biosensors based on choline oxidase entrapped in polyacrylamide microgels, *Electroanalysis* 19 (2007) 370–378.
- [6] H. Zhang, Y. Yin, P. Wu, C. Cai, Indirect electrocatalytic determination of choline by monitoring hydrogen peroxide at the choline oxidase-prussian blue modified iron phosphate nanostructures, *Biosens. Bioelectron.* 31 (2012) 244–250.
- [7] F. Ricci, A. Amine, G. Palleschi, D. Moscone, Prussian blue based screen printed biosensors with improved characteristics of long-term lifetime and pH stability, *Biosens. Bioelectron.* 18 (2003) 165–174.
- [8] H. Shi, Y. Yang, J. Huang, Z. Zhao, Amperometric choline biosensors prepared by layer-by-layer deposition of choline oxidase on the prussian blue-modified platinum electrode, *Talanta* 70 (2006) 852–858.
- [9] Z. Song, J. D. Huang, B. Y. Wu, H. B. Shi, J. I. Anzai, Q. Chen, Amperometric aqueous sol-gel biosensor for low-potential stable choline detection at multi-wall carbon nanotube modified platinum electrode, *Sensor Actuat. B-Chem.* 115 (2006) 626–633.
- [10] A.H. Keihan, S. Sajjadi, N. Sheibani, A.A. Moosavi-Movahedi, A highly sensitive choline biosensor based on bamboo-like multiwall carbon nanotubes/ionic liquid/Prussian blue nanocomposite, *Sensor Actuat. B-Chem.* 204 (2014) 694–703.
- [11] S. Sajjadi, H. Ghourchian, H.A. Rafiee-Pour, P. Rahimi, Accelerating the electron transfer of choline oxidase using ionic-liquid/NH<sub>2</sub>-MWCNTs nano-composite, *J. Iran Chem. Soc.* 9 (2012) 111–119.
- [12] K. Deng, J. Zhou, X. Li, Noncovalent nanohybrid of ferrocene with chemically reduced graphene oxide and its application to dual biosensor for hydrogen peroxide and choline, *Electrochim. Acta* 95 (2013) 18–23.
- [13] Y.H. Bai, Y. Du, J. J. Xu, and H. Y. Chen, Choline biosensors based on a bi-electrocatalytic property of MnO<sub>2</sub> nanoparticles modified electrodes to H<sub>2</sub>O<sub>2</sub>, *Electrochem. Comm.* 9 (2007) 2611–2616.

- [14] M. Belesi, I. Panagiotopoulos, S. Pal, S. Hariharan, D. Tsi trouli, G. Papavassiliou, D. Niarchos, N. Boukos, M. Fardis, V. Tzitzios, Decoration of carbon nanotubes with CoO and Co nanoparticles, *J. Nanomater.* ID 320516 (2011).
- [15] F. Qu, M. Yang, J. Jiang, G. Shen, R. Yu, Amperometric biosensor for choline based on layer-by-layer assembled functionalized carbon nanotube and polyaniline multilayer film, *Anal. Biochem.* 344 (2005) 108–114.
- [16] S. Pundir, N. Chauhan, J. Narang, C.S. Pundir, Amperometric choline biosensor based on multiwalled carbon nanotubes/zirconium oxide nanoparticles electrodeposited on glassy carbon electrode, *Anal. Biochem.* 427 (2012) 26–32.
- [17] S.S. Razola, S. Pochet, K. Grosfils, J.M. Kauffmann, Amperometric determination of choline released from rat submandibular gland acinar cells using a choline oxidase biosensor, *Biosens. Bioelectron.* 18 (2003) 185–191.
- [18] P. Rahimi, H. Ghourchian, S. Sajjadi, Effect of hydrophilicity of room temperature ionic liquids on the electrochemical and electrocatalytic behavior of choline oxidase, *Analyst* 137 (2012) 471–475.
- [19] B.Y. Wu, S.H. Hou, F. Yin, Z.-X. Zhao, Y.Y. Wang, X.S. Wang, Q. Chen, Amperometric glucose biosensor based on multilayer films via layer-by-layer selfassembly of multi-wall carbon nanotubes, gold nanoparticles and glucose oxidase on the Pt electrode, *Biosens. Bioelectron.* 22 (2007) 2854–2860.
- [20] S. Hrapovic, Y. Liu, K. B. Male, and J. H. T. Luong, Electrochemical biosensing platforms using platinum nanoparticles and carbon nanotubes, *Anal. Chem.* 76 (2004) 1083–1088.
- [21] C. Wang, G. Wang, and B. Fang, Electrocatalytic oxidation of bilirubin at ferrocenecarboxamide modified MWCNT-gold nanocomposite electrodes, *Microchim. Acta* 164 (2009) 113–118.
- [22] B.Y. Wu, S.H. Hou, F. Yin, J. Li, Z.-X. Zhao, J.-D. Huang, Q. Chen, Amperometric glucose biosensor based on layer-by-layer assembly of multilayer films composed of chitosan, gold nanoparticles and glucose oxidase modified Pt electrode, *Biosens. Bioelectron.* 22 (2007) 838–844.

- [23] V. Pavlov, Y. Xiao, I. Willner, Inhibition of the acetylcholine esterase-stimulated growth of Au nanoparticles: nanotechnology-based sensing of nerve gases, *Nano Lett.* 5 (2005) 649–653.
- [24] D.N. Ventura, R.A. Stone, K.-S. Chen, H.H. Hariri, K.A. Riddle, T.J. Fellers, C.S. Yun, G.F. Strouse, H.W. Kroto, S.F.A. Acquah, Assembly of cross-linked multi-walled carbon nanotube mats, *Carbon* 48 (2010) 987–994.
- [25] X. Hu, T. Wang, X. Qu, S. Dong, In situ synthesis and characterization of multiwalled carbon nanotube/Au nanoparticle composite materials, *J. Phys. Chem. B* 110 (2006) 853–857.
- [26] H. Zhang, Z. Meng, Q. Wang, J. Zheng, A novel glucose biosensor based on direct electrochemistry of glucose oxidase incorporated in biomediated gold nanoparticles carbon nanotubes composite film, *Sensor Actuat. B-Chem.* 158 (2011) 23–27.
- [27] B. Wu, Z. Ou, X. Ju, S. Hou, Carbon nanotubes/gold nanoparticles composite film for the construction of a novel amperometric choline biosensor, *J. Nanomater.* ID 464919 (2011).
- [28] X. Qin, H. Wang, X. Wang, Z. Miao, L. Chen, W. Zhao, M. Shan, Q. Chen, Amperometric biosensors based on gold nanoparticles-decorated multiwalled carbon nanotubes poly(diallyldimethylammonium chloride) biocomposite for the determination of choline, *Sensor Actuat. B-Chem.* 147 (2010) 593–598.
- [29] S.K. Roy, M.E. Orazem, Analysis of flooding as a stochastic process in polymer electrolyte membrane (PEM) fuel cells by impedance techniques, *J. Power Sources* 184 (2008) 212–219.
- [30] J.S. Daniels, N. Pourmand, Label-free impedance biosensors: Opportunities and challenges, *Electroanalysis* 19 (2007) 1239–1257.
- [31] A. Bonanni, A.H. Loo, M. Pumera, Graphene for impedimetric biosensing, *Trac-Trends Anal. Chem.* 37 (2012) 12–21.
- [32] S.-R. Lee, H.-E. Lee, Y.O. Kang, H.-S. Hwang, S.-H. Choi, Bionzymatic acetylcholinesterase and choline oxidase immobilized biosensor based on a phenyl carboxylic acid-grafted multiwalled carbon nanotube, *Adv. Mat. Sci. Eng.* ID 971942 (2014).
- [33] M.E. Ghica, R. Pauliukaite, O. Fatibello-Filho, C.M.A. Brett, Application of functionalised carbon nanotubes immobilised into chitosan films in amperometric enzyme biosensors, *Sensor Actuat. B-Chem.* 142 (2009) 308-315.

- [34] D. Aili, K. Enander, J. Rydberg, I. Nesterenko, F. Bjorefors, L. Baltzer, B. Liedberg, Folding induced assembly of polypeptide decorated gold nanoparticles, *J. Am. Chem. Soc.* 130 (2008) 5780–5788.
- [35] M.N. Tchoul, W.T. Ford, G. Lolli, D.E. Resasco, S. Arepalli, Effect of mild nitric acid oxidation on dispersability, size, and structure of single-walled carbon nanotubes, *Chem. Mater.* 19 (2007) 5765–5772.
- [36] T. Shimomura, T. Itoh, T. Sumiya, F. Mizukami, M. Ono, Amperometric determination of choline with enzyme immobilized in a hybrid mesoporous membrane, *Talanta* 78 (2009) 217-220.
- [37] L. Zhang, J. Chen, Y. Wang, L. Yu, J. Wang, H. Peng, J. Zhu, Improved enzyme immobilization for enhanced bioelectrocatalytic activity of choline sensor and acetylcholine sensor, *Sensor Actuat. B-Chem.* 193 (2014) 904–910.
- [38] H.-C. Chen, R.-Y. Tsai, Y.-H. Chen, R.-S. Lee, M.-Y. Hua, A colloidal suspension of nanostructured poly(N-butyl benzimidazole)-graphene sheets with high oxidase yield for analytical glucose and choline detections, *Anal. Chim. Acta* 792 (2013) 101-109.
- [39] M. Shamsipur, S.H. Kazemi, M.F. Mousavi, Impedance studies of a nano-structured conducting polymer and its application to the design of reliable scaffolds for impedimetric biosensors, *Biosens. Bioelectron.* 24 (2008) 104–110.
- [40] M. Shamsipur, M. Asgari, M.F. Mousavi, R. Davarkhah, A novel hydrogen peroxide sensor based on the direct electron transfer of catalase immobilized on nano-sized NiO/MWCNTs composite film, *Electroanalysis* 24 (2012) 357–367.
- [41] J.L.F.C. Lima, C. Delerue-Matos, M. Carmo V. F. Vaz, Enzymatic determination of choline in milk using a FIA system with potentiometric detection, *Analyst* 125 (2000) 1281-1284.

### Figure captions

**Figure 1.** Schematic diagram illustrating possible links formed after enzyme immobilisation at the electrode modified with MWCNT, chitosan and GNP.

**Figure 2.** (A) Transmission electron microscopy of (a1) MWCNT, (a2) GNP, (a3) MWCNT/GNP; (B) UV-Vis spectra of (—) MWCNT, (— · — · —) GNP and (-----) MWCNT/GNP.

**Figure 3.** Effect of: (A) applied potential on the response to 33  $\mu\text{M}$  choline; (B) ChOx concentration on the biosensor sensitivity at  $-0.3\text{ V}$ ; (C) pH value on the response to 20  $\mu\text{M}$  choline at  $\text{ChOx}/(\text{GNP})_4/\text{MWCNT}/\text{GCE}$ . (A) and (B) in 0.1 M NaPBS, pH 8.5.

**Figure 4.** Calibration plot for choline amperometric determination in 0.1 M NaPBS, pH 8.5 at  $-0.3\text{ V}$  for different biosensor configurations.

**Figure 5.** (A) Complex plane impedance spectra for: ( $\blacktriangle$ )  $\text{ChOx}/\text{GNP}/\text{GCE}$ , ( $\circ$ )  $\text{ChOx}/\text{GO}/\text{GCE}$ , ( $\bullet$ )  $\text{ChOx}/\text{RG}/\text{GCE}$ , ( $\Delta$ )  $\text{ChOx}/\text{MWCNT}/\text{GCE}$ , ( $\blacksquare$ )  $\text{ChOx}/\text{GNP}/\text{MWCNT}/\text{GCE}$ , at 0.0 V vs Ag/AgCl in 0.1 M NaPBS pH 8.5; (B) Equivalent electrical circuit used to fit the spectra.

**Figure 6.** (A) Complex plane impedance spectra at  $\text{ChOx}/(\text{GNP})_4/\text{MWCNT}/\text{GCE}$  in 0.1 M NaPBS pH 8.5, with different choline concentrations from 1 to 500  $\mu\text{M}$ ; (B) Calibration plot of  $-Z''$  vs. logarithm of choline concentration at frequency 0.1 Hz.

## FIGURES

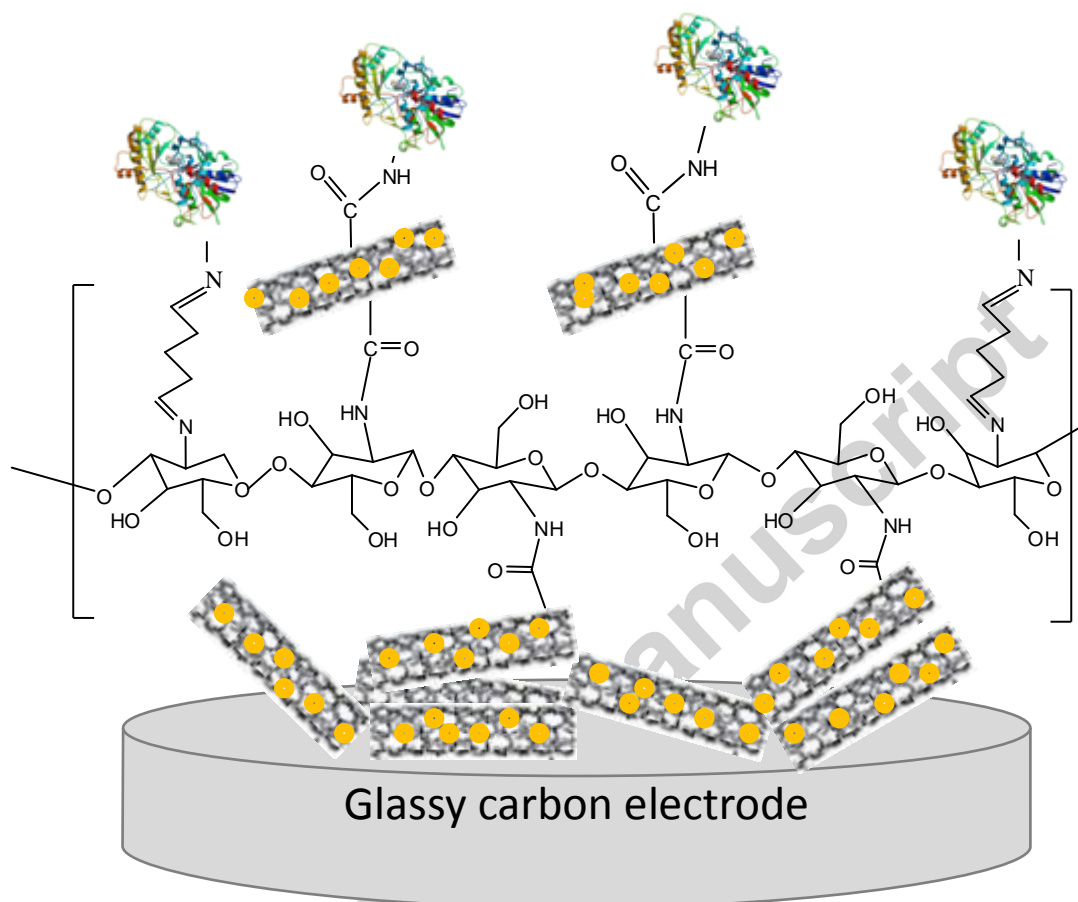
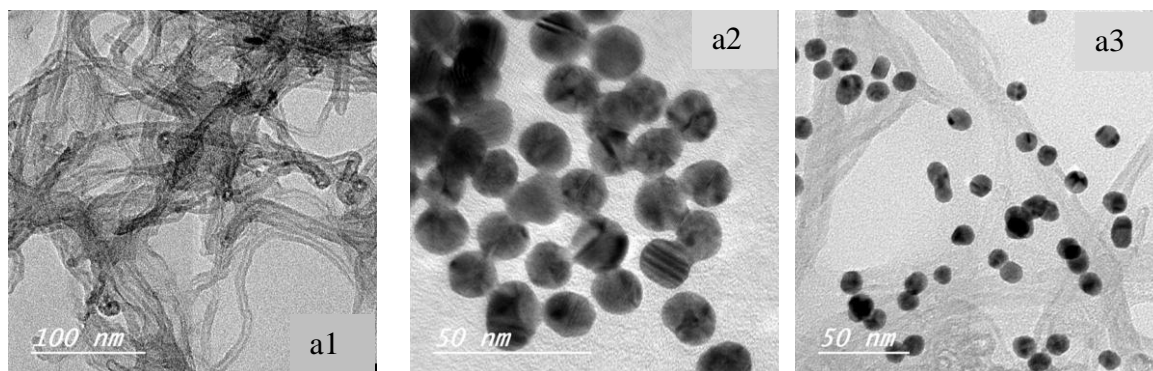


**Figure 1.** Schematic diagram illustrating possible links formed after enzyme immobilisation at the electrode modified with MWCNT, chitosan and GNP.

(A)



(B)

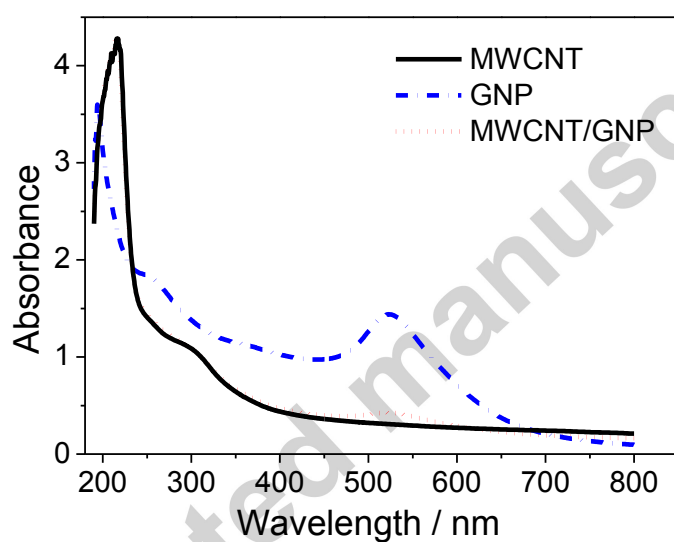


**Figure 2.** (A) Transmission electron microscopy of (a1) MWCNT, (a2) GNP, (a3) MWCNT/GNP; (B) UV-Vis spectra of (—) MWCNT, (---) GNP and (.....) MWCNT/GNP.

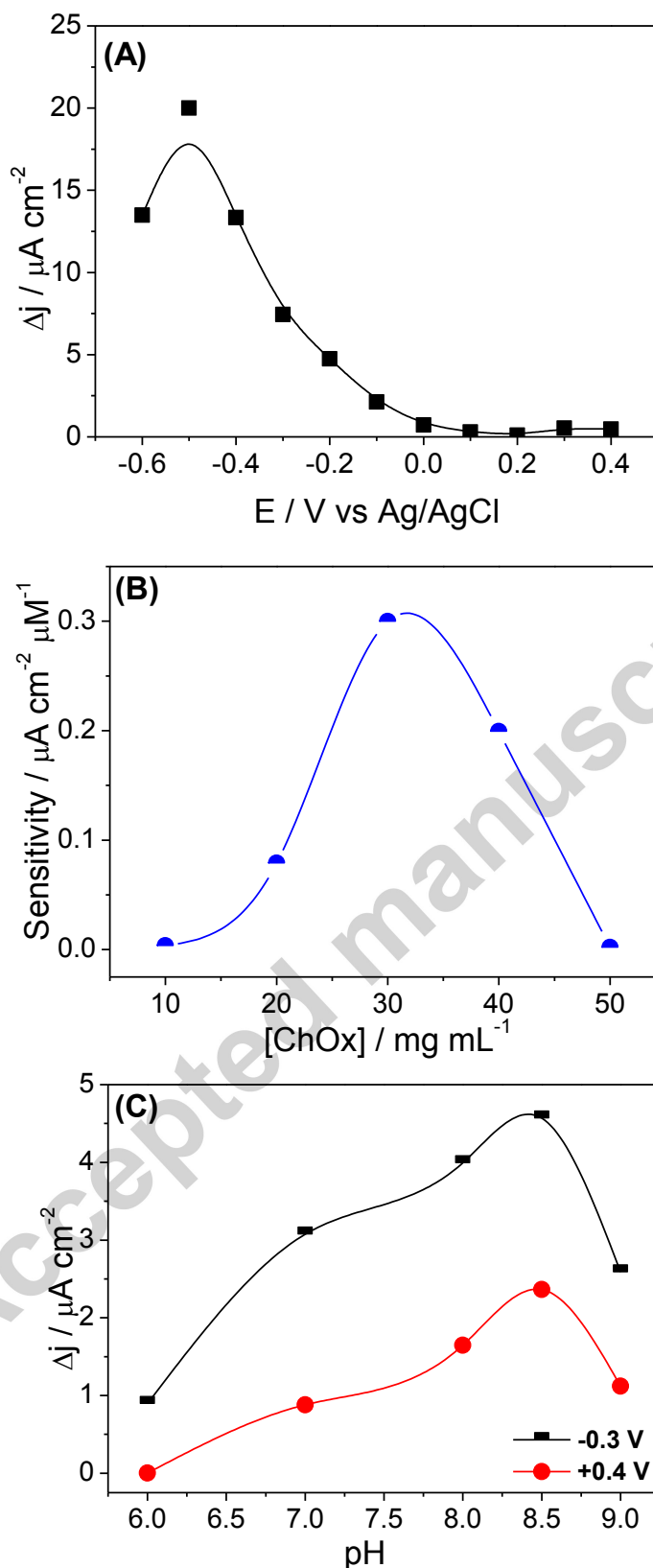


**Figure 3.** Effect of (A) applied potential on the response to 33  $\mu\text{M}$  choline; (B) ChOx concentration on the biosensor sensitivity at  $-0.3 \text{ V}$ ; (C) pH value on the response to 20  $\mu\text{M}$  choline at ChOx/(GNP)<sub>4</sub>/MWCNT/GCE. (A) and (B) in 0.1 M NaPBS, pH 8.5.



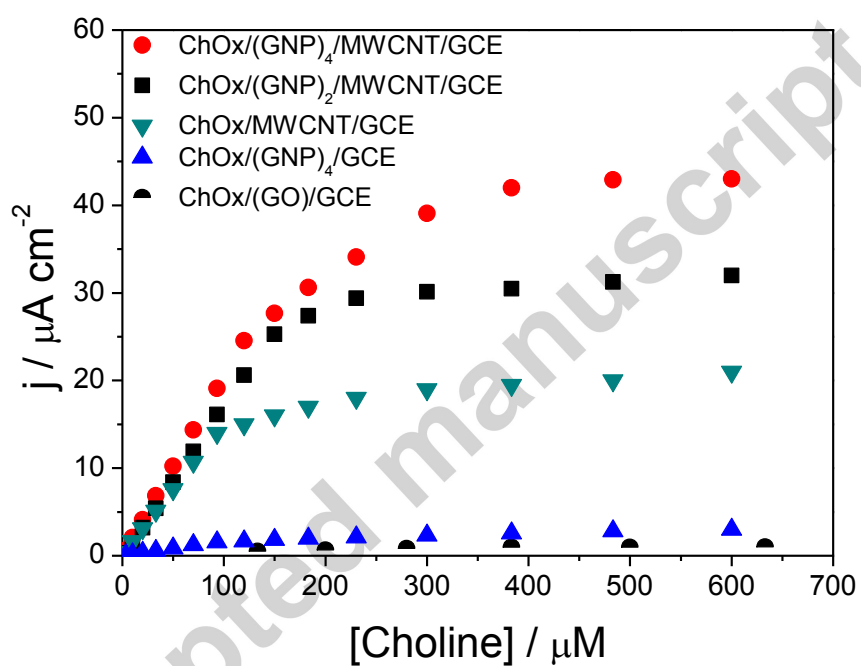
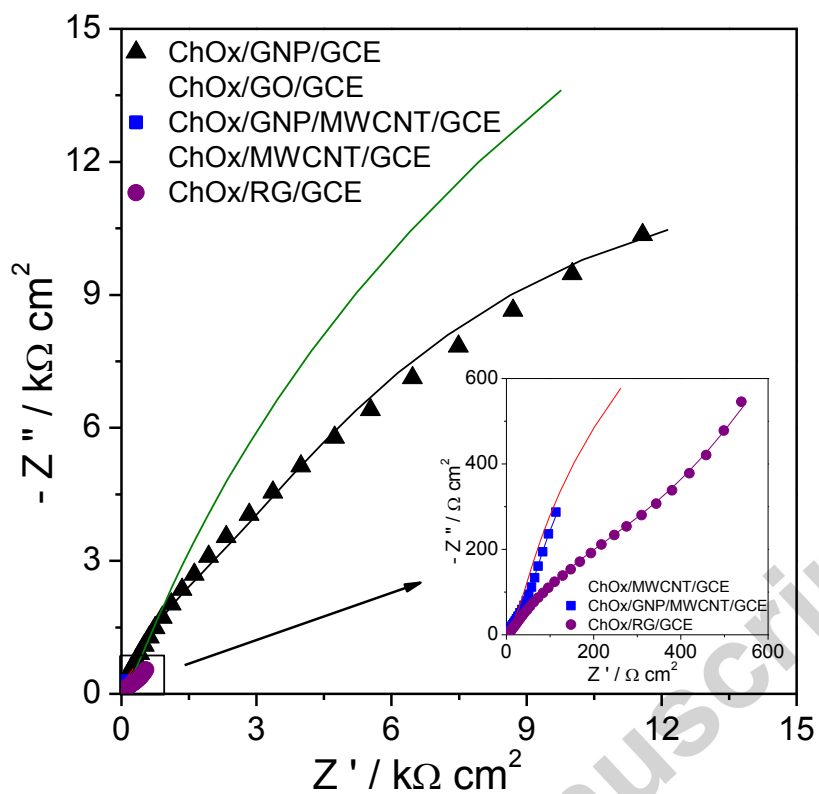


**Figure 4.** Calibration plot for choline amperometric determination in 0.1 M NaPBS, pH 8.5 at -0.3 V for different biosensor configurations.

(A)



(B)

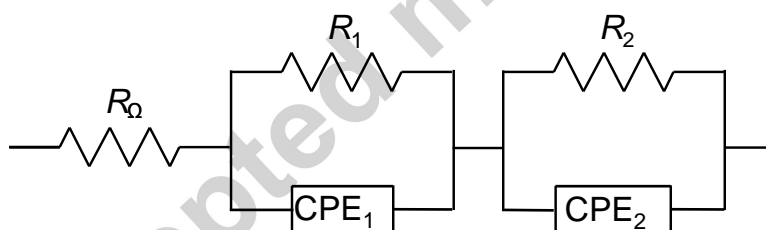


**Figure 5.** (A) Complex plane impedance spectra for: (▲) ChOx/GNP/GCE, (○) ChOx/GO/GCE, (●) ChOx/RG/GCE, (△) ChOx/MWCNT/GCE, (■) ChOx/(GNP)<sub>4</sub>/MWCNT/GCE at 0.0 V vs Ag/AgCl in 0.1 M NaPBS pH 8.5; (B) Equivalent electrical circuit used to fit the spectra.

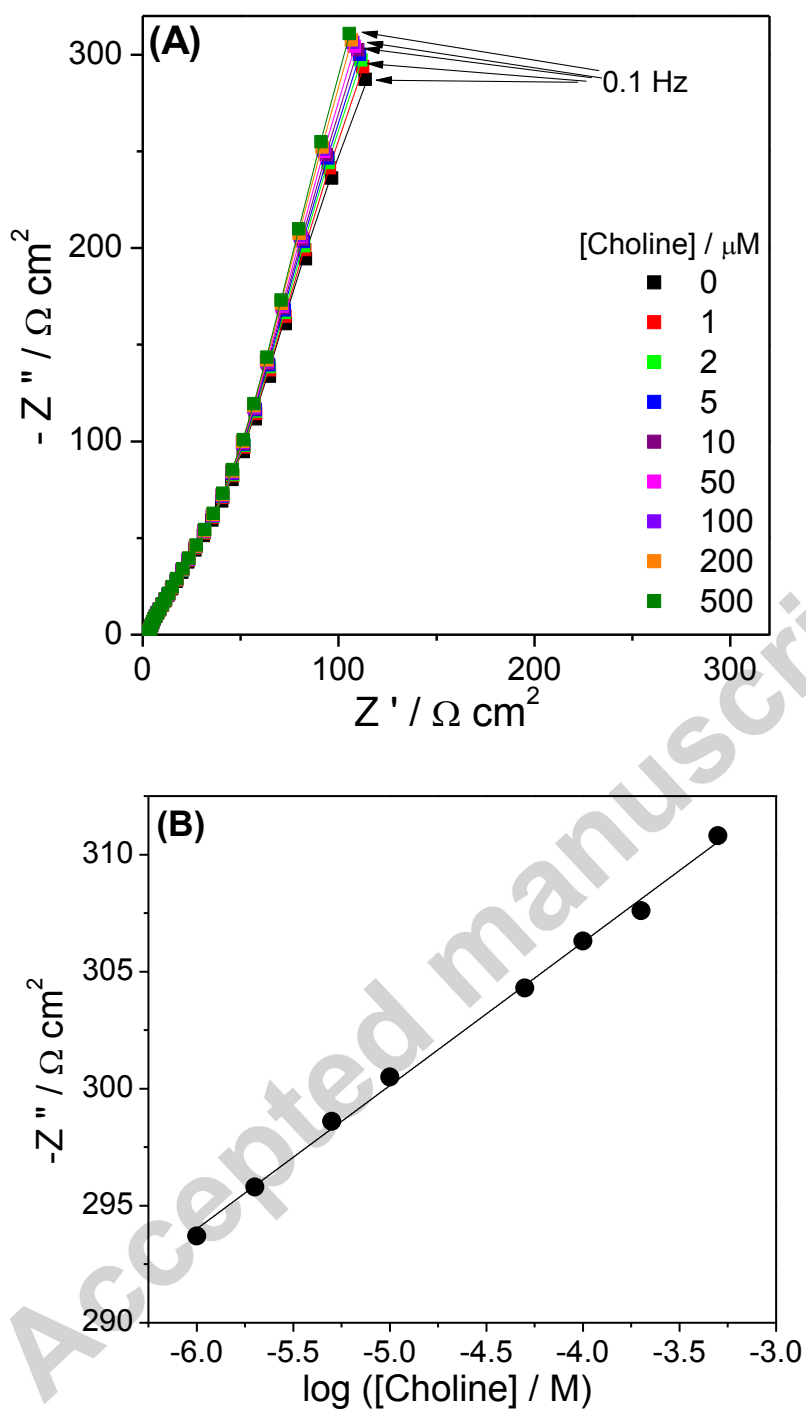


**Figure 6.** (A) Complex plane impedance spectra at  $\text{ChOx}/(\text{GNP})_4/\text{MWCNT}/\text{GCE}$  in 0.1 M NaPBS pH 8.5, with different choline concentrations from 1 to 500  $\mu\text{M}$ ; (B) Calibration curve of  $-Z''$  vs. logarithm of choline concentration at frequency 0.1 Hz.

## Tables

**Table 1.** Electroanalytical performance of different choline biosensors by fixed-potential amperometry at - 0.3 V vs Ag/AgCl.

Modified electrode	Linear range / $\mu\text{M}$	Sensitivity / $\mu\text{A cm}^{-2} \text{mM}^{-1}$	LoD / $\mu\text{M}$
ChOx/GO/GCE	133-480	1.79	41
ChOx/(GNP) <sub>2</sub> /GCE	3-90	16.7	4.2
ChOx/MWCNT/GCE	3-90	150	2.2
ChOx/(GNP) <sub>2</sub> /MWCNT/GCE	3-150	172	3.3
ChOx/(GNP) <sub>4</sub> /MWCNT/GCE	3-120	204	0.6

**Table 2.** Comparison of electroanalytical parameters of the proposed biosensor with other reported choline biosensors.

Biosensor	Potential / V	Buffer pH	Linear range / $\mu\text{M}$	Sensitivity / $\mu\text{A cm}^{-2} \text{mM}^{-1}$	LoD / $\mu\text{M}$	Ref.
ChOx/PDDA/PB-FePO <sub>4</sub> /GCE	-0.05 (SCE)	8.0	2-3200	75.2	0.4	6
ChOx/PB/SPE	-0.05 (Ag-SPE)	7.4	0.5-100	110	0.5	7
ChOx/PB/PtE	0.0 (Ag/AgCl)	7.4	0.5-100	88.6	0.5	8
ChOx/MWCNT/PtE	+0.16 (Ag/AgCl)	7.4	5-100	133	0.1	9
ChOx/Ni-PB/MWCNT-IL//GCE	-0.05 (Ag/AgCl)	7.4	0.45-100	345.4	0.45	10
ChOx/IL/MWCNT/GCE	-0.395 (Ag/AgCl)	7.0	6.9-670	82.5	2.7	11
ChOx/HRP/Fc-CRGO/GCE	-0.1 (SCE)	7.4	1-400	*	0.35	12
ChOx/(CNT/PANI) <sub>5</sub> /(PANI) <sub>3</sub> /GCE	+0.4 (SCE)	6.98	1-2000	1.39	0.3	15

ChOx- AChE/MWCNT/ZrO <sub>2</sub> NP/GCE	+0.15 (Ag/AgCl)	7.4	0.05–1	*	0.01	16
ChOx/HRP-PHZ-CPE	0.0 (Ag/AgCl)	7.4	0.5-70	11.73	0.1	17
ChOx/IL/NH <sub>2</sub> -MWCNT/GCE	-0.45 (Ag/AgCl)	7.0	5-800	125.8	3.85	18
ChOx/GNP/MWCNT/PtE	+0.6 (Ag/AgCl)	8.0	50-800	*	15	27
ChOx-PDDA-GNP-MWCNT/PtE	+0.35 (Ag/AgCl)	7.6	1-500	183	0.3	28
PDDA/ChOx/ZnO/MWCNT/PGE	+0.4 (Ag/AgCl)	7.8	1-800	178	0.3	37
ChOx/PBBI-Gs/Au	-0.5 (Ag/AgCl)	6.4	0.1-830	494	0.02	38
ChOx/(GNP) <sub>4</sub> /MWCNT/GCE	-0.3 (Ag/AgCl)	8.5	3.3–120	204	0.6	This work

LoD - limit of detection, ChOx - choline oxidase, AChE - acetylcholine esterase, HRP - horseradish peroxidase, PB - Prussian blue, PANI - polyaniline, PDDA - poly(diallyldimethylammonium), PHZ - phenothiazine, PBBI - poly(N-butyl benzimidazole), ZrO<sub>2</sub>NP - ZrO<sub>2</sub> nanoparticle, GNP - gold nanoparticles, Fc - ferrocene, CRGO - chemically reduced graphene oxide, Gs - graphene sheets, IL - ionic liquid, NH<sub>2</sub>-MWCNT - aminofunctionalised MWCNT, CPE - carbon paste electrode, SPE - screen printed electrode, PtE - platinum electrode, GCE - glassy carbon electrode, PGE - pyrolytic graphite electrode, \* - no electrode area provided

**Table 3.** Values of equivalent circuit parameters from fitting of the impedance spectra in Fig. 5A, for different electrode configurations in 0.1 M NaPBS, pH 8.5 at 0.0 V vs. Ag/AgCl.

Value of  $R_{\Omega}$   $\sim 2.7 \Omega \text{ cm}^2$ .

	$C_1 /$ $\text{mF cm}^{-2} \text{ s}^{\alpha-1}$	$\alpha_1$	$R_1 /$ $\Omega \text{ cm}^2$	$C_2 /$ $\text{mF cm}^{-2} \text{ s}^{\alpha-1}$	$\alpha_2$	$R_2 /$ $\text{k}\Omega \text{ cm}^2$
ChOx/GO/GCE	0.028	0.96	150	0.043	0.78	58.4
ChOx/RG/GCE	1.19	0.64	410	1.10	0.68	0.004
ChOx/(GNP) <sub>2</sub> /GCE	0.032	0.83	1575	0.029	0.84	23.7
ChOx/MWCNT/GCE	7.23	0.67	36.8	2.80	0.92	2.49
ChOx/(GNP) <sub>4</sub> /MWCNT/GCE	5.30	0.73	62.5	5.30	0.96	2.04

Accepted manuscript

**Table 4.** Values of equivalent circuit parameters from fitting of the impedance spectra in Fig. 6A for ChOx/(GNP)<sub>4</sub>/MWCNT/GCE in 0.1 M NaPBS, pH 8.5 at 0.0 V vs. Ag/AgCl. Value of  $R_{\Omega}$   $\sim$ 2.7  $\Omega$  cm<sup>2</sup>.

	$C_1 /$ mF cm <sup>-2</sup> s <sup><math>\alpha_1</math></sup>	$\alpha_1$	$R_1 /$ $\Omega$ cm <sup>2</sup>	$C_2 /$ mF cm <sup>-2</sup> s <sup><math>\alpha_2</math></sup>	$\alpha_2$	$R_2 /$ k $\Omega$ cm <sup>2</sup>
Buffer	5.30	0.73	62.5	5.30	0.96	2.04
+ 1 $\mu$ M Choline	5.32	0.73	60.9	5.15	0.95	2.55
+ 2 $\mu$ M Choline	5.31	0.73	59.4	5.07	0.94	2.81
+ 5 $\mu$ M Choline	5.32	0.73	58.8	5.02	0.94	2.91
+ 10 $\mu$ M Choline	5.31	0.73	58.7	5.00	0.94	3.09
+ 50 $\mu$ M Choline	5.33	0.73	57.8	4.95	0.94	3.38
+100 $\mu$ M Choline	5.31	0.73	57.4	4.93	0.94	3.50
+ 200 $\mu$ M Choline	5.30	0.73	58.0	4.92	0.94	3.63
+ 500 $\mu$ M Choline	5.28	0.73	57.8	4.87	0.94	4.02

#### Highlights

- Novel amperometric biosensor for choline determination using choline oxidase
- Biosensor architecture incorporates carbon nanotubes and gold nanoparticles
- Linear response range up to 120  $\mu$ M and detection limit 0.6  $\mu$ M
- Electrochemical impedance spectroscopy also used to measure choline

Successful measurement of choline in milk samples